Orientation of Cobalt-Phthalocyanines on Molybdenum disulfide: Distinguishing between Single Crystals and Small Flakes

Philipp Haizmann[1,#], Eric Juriatti[1,#], Maren Klein[1], Katharina Greulich[1], Peter Nagel[2], Michael Merz[2], Stefan Schuppler[2], Amir Ghiami[2], Ruslan Ovsyannikov[3], Erika Giangrisostomi[3], Thomas Chassé[1], Marcus Scheele[1,], Heiko Peisert[1,*]*

1 Institut für Physikalische und Theoretische Chemie, Universität Tübingen, 72076 Tübingen, Germany

2 Institute for Quantum Materials and Technologies (IQMT), Karlsruhe Institute of Technology (KIT), 76021 Karlsruhe, Germany, and Karlsruhe Nano and Micro Facility (KNMFi), Karlsruhe Institute of Technology, 76344 Eggenstein-Leopoldshafen, Germany

3 Institute for Methods and Instrumentation for Synchrotron Radiation Research, Helmholtz-Zentrum Berlin für Materialien und Energie GmbH, 12489 Berlin, Germany

[#] These authors contributed equally.

* Corresponding author, heiko.peisert@uni-tuebingen.de, Tel.: (+49) 07071 / 29-76931, Fax: (+49) 07071 / 29-5490 and marcus.scheele@uni-tuebingen.de

Abstract

Heterostructures consisting of transition metal dichalcogenides (TMDCs) and organic molecules are currently of enormous interest for a variety of applications. Comparably weakly interacting molecules like phthalocyanines exhibit a high potential for the tuning of electronic properties of TMDCs. Knowledge of the molecular orientation is a prerequisite for the understanding of the nature and strength of the interfacial interaction. We study the molecular orientation of cobalt phthalocyanine (CoPc) and perfluorinated ($CoPcF_{16}$) on both large molybdenum disulfide (MoS_2) single crystals and small MoS_2 flakes using synchrotron-based techniques: X-ray absorption spectroscopy (XAS) at the Co L_3 edge and spectromicroscopy in a photoemission electron microscope (PEEM). We show that the orientation can be radically different on both substrates. Whereas on large crystals an almost flat-lying orientation is observed, significant tilt angles were found on smaller flakes. The orientation depends crucially on the number of MoS_2 layers and/or the size of flat terraces.

TOC GRAPHICS

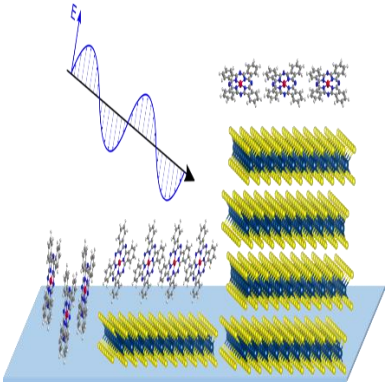

KEYWORDS

X-Ray absorption spectroscopy (XAS), photo emission electron spectroscopy (PEEM), Functionalization, Work function, Heterojunctions

Due to their remarkable physical and chemical properties, layered transition metal dichalcogenides (TMDCs) have emerged as promising materials for applications in modern semiconductor devices for electronics, lighting, solar energy and communication. In particular, it is expected that these materials will enable the further miniaturization of electronic devices according to Moore's law,[1, 2] and promote the establishment of flexible electronic devices.[3] The layered structure allows the exfoliation down to two-dimensional layers with unique electronic properties compared to their bulk counterparts; in the case of MoS_2, the nature of the band gap changes from direct to indirect.[4-6] Especially TMDC monolayers and heterostructures are of interest for a broad variety of devices.[2, 7-9]

One approach for the tuning of electronic properties is the formation of TMDC/organic semiconductor heterostructures. The recent research on conjugated carbon molecule/TMDC interfaces has been mainly focused on strong molecular electron acceptors.[10-13] However, also weaker interacting, physiosorbed carbon molecules may also interact with TMDCs. Such systems are expected to offer new opportunities for tuning both optical and electronic characteristics.[14] For example, a quenching of the low-temperature defect photoluminescence of MoS_2 was observed after adsorption of metal-phthalocyanines, depending strongly on the central metal atom of the phthalocyanine.[15] The nature of such interactions is currently increasingly discussed,[16] and one crucial parameter in this regard is the orientation of the molecules with respect to the substrate surface. For example, the coupling between nickel phthalocyanine (NiPc) and graphene is supported by the flat geometry of the NiPc complexes.[17] Especially for anisotropic organic semiconductor films, the orientation of the individual molecules at the heterostructure is of particular significance since it influences the electronic properties of the film and therefore the overall interaction at the interface.[18, 19]

We study the molecular orientation of cobalt phthalocyanine (CoPc) and perfluorinated cobalt phthalocyanine ($CoPcF_{16}$) on MoS_2 bulk crystals and on exfoliated pieces, often called flakes, which have fewer and even monolayer thickness – a system, where weak interactions at

interfaces (i.e. the absence of an integer charge transfer) can be expected. Representatives of the family of transition metal phthalocyanines (TMPcs) were chosen due to their advantageous chemical and physical properties, including stability, film growth and tunability of electronic parameters due to variation of the central metal and selection of the peripheral substituents.[20-23] Fluorination of the Pc moiety increases the ionization energy by more than 1 eV,[24-27] which may affect electronic interactions at interfaces distinctly - even in the case of metal surfaces passivated by graphene.[28] Numerous studies on the growth of phthalocyanines were carried out on a broad variety of substrates. On single crystalline substrates, the almost planar phthalocyanine molecules typically prefer a flat-lying orientation (see, e.g.[20, 29-35]); this includes also van der Waals substrates like GeS or MoS_2 and graphene covered metal substrates.[30, 32-35] In contrast, on polycrystalline substrates, the molecular orientation can be radically different depending crucially on the substrate roughness.[29, 30] The different growth modes observed on various substrates can be understood in terms of different molecule-substrate and molecule-molecule interactions at the interface.[29, 36-38] In this manner, higher tilt-angles for phthalocyanines on single crystals were in particular found, if the molecule-substrate interaction is weaker, e.g. for van-der-Waals solids or passivated semiconductor surfaces.[32, 39]

In this study, we demonstrate that the orientation of CoPc and $CoPcF_{16}$ on molybdenum disulfide flakes can diverge from that on the bulk single crystal. Therefore, the prediction of the molecular orientation on thin flakes from literature data obtained with bulk crystals only could be misleading for differing structural situations.

Polarization-dependent X-ray absorption spectroscopy (XAS) offers an optimal method for studying the adsorption geometry of molecular adsorbates.[29, 40] For the planar TMPcs having D_{4h} symmetry, both C1s-π* or N1s-π* excitations are suitable for determining molecular orientation.[29] If the electric field vector of the incoming light is oriented parallel to the atomic p_z wave functions forming the molecular π* orbital (i.e. out of the molecular plane), the absorption is maximal, whereas the transition is forbidden in the case of a perpendicular

orientation.[40, 41] However, in our case the analysis of both C K and N K edge absorption spectra is hindered by the overlap with features from the MoS_2 substrate and common carbon contaminations. An example for an N K edge spectrum in superposition with Mo $M_{3,2}$ is shown in **Figure S1** (supporting information). However, also Co L edge XAS spectra show a pronounced angular dependence (see, e.g. Refs.[34, 42]). They are determined to a large extent by multiplet effects due to the strong overlap between core level and valence wave functions.[43] Nevertheless, in-plane and out-of-plane transitions can be distinguished (for details we refer to the literature, e.g. Refs. [44, 45]). In the following, we will use the shape of the Co L_3 XAS spectra for the estimation of the molecular orientation. We note that the shape of these spectra is almost independent on the fluorination of CoPc (cf., e.g. Refs [34, 46]).

In **Figure 1**, polarization dependent Co L_3 edge spectra of (**Fig 1a**) $CoPcF_{16}$ and (**Fig 1b**) CoPc on bulk MoS_2 are shown for two different film thicknesses, measured at two different incidence angles of the p-polarized light. Transitions polarized perpendicular to the molecular plane (z-polarized) are denoted A, whereas B features are polarized within the molecular plane (xy-polarized). Consistent with the considerations above, the intensity of the out-of-plane feature A is maximal at grazing incidence (20°), whereas the in-plane transitions B are most intense at normal incidence (90°). This indicates a preferred orientation of the molecule parallel to the substrate surface. The spectral shape of the Co L_3 edge is almost identical for the coverage in the monolayer range (0.34 nm) and the multilayer film, indicating that the orientation of the first molecular layer is maintained in the thin film. This behavior on bulk MoS_2 substrates is identical for CoPc and $CoPcF_{16}$. A more detailed comparison of the spectral shapes in **Figure 1** with literature data (e.g. Refs. [34, 42, 46]) reveals that tilt angles between the molecules and the substrate surface are rather small or even negligible. Thus, we can conclude that the face-on orientation of CoPc and $CoPcF_{16}$ is favored on bulk MoS_2.

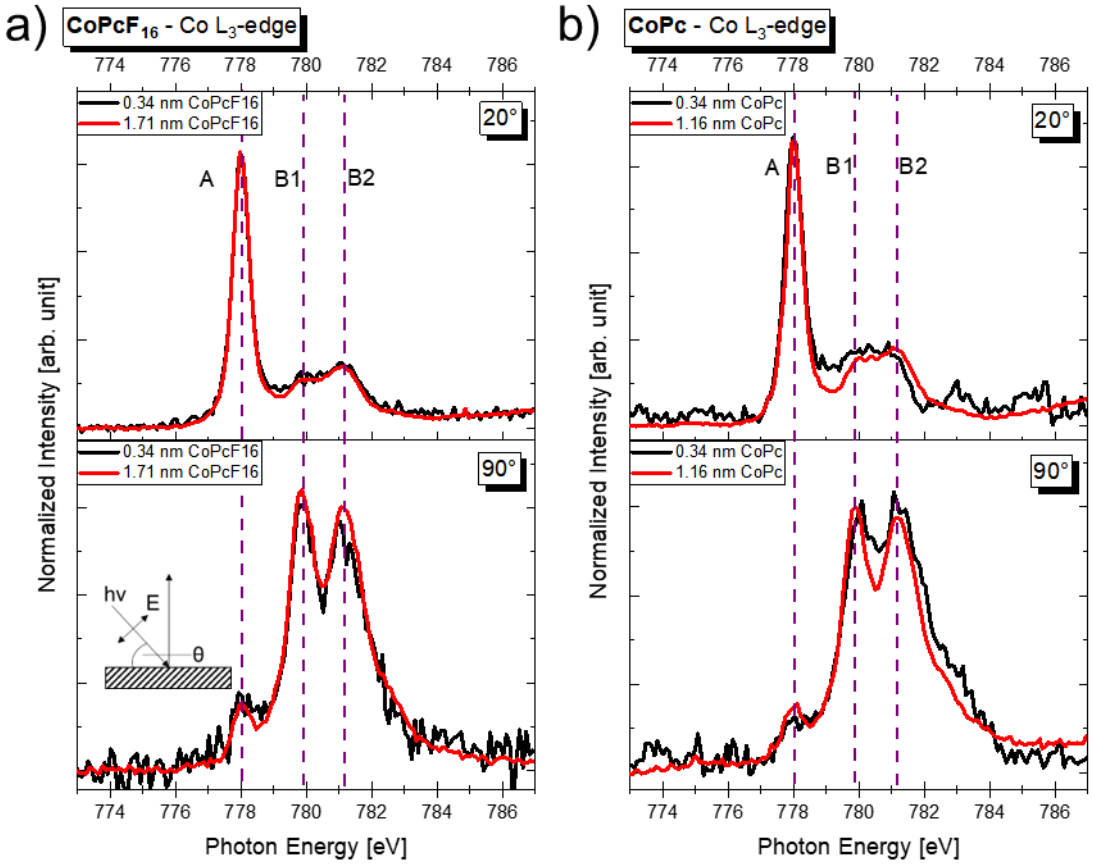

Figure 1 Angle-dependent measurements in the Co L_3 region show intensity differences of features A and the two B features depending on the orientation of the electric field with respect to the sample for $CoPcF_{16}$ shown in a) and CoPc shown in b).

While the molecular orientation on bulk MoS_2 provides critical insight, it's essential to recognize that this orientation could be influenced by numerous factors on real MoS_2 samples like, e.g. 2D layers or flakes. For instance, the substrate's surface roughness and the size of its atomically flat terraces can significantly impact the direction of molecules.[29] This leads to the question if the determined molecular orientation of cobalt phthalocyanines on bulk MoS_2 applies also to smaller flakes, which are of particular interest for applications. Due to the small dimensions of the MoS_2 flakes, a microscopic technique is needed. A certain PEEM measurement mode, spectromicroscopy, is particularly useful here. Spectromicroscopy essentially means taking stacks of PEEM images while scanning the incoming photon energy or the kinetic energy of the emitted electrons; by tracing a pixel (or lateral region) through the

image stack the former yields laterally resolved (μ-)XAS, the latter laterally resolved (μ-)PES. The resulting local spectra can be summed over regions of interest (RoI's) with freely defined shapes as applied on measurements discussed in the following. In particular, microscopic measurements of the work function contrast have proven to be a very sensitive method for distinguishing monolayer and few-layer regions of TMDC flakes.[47-49]

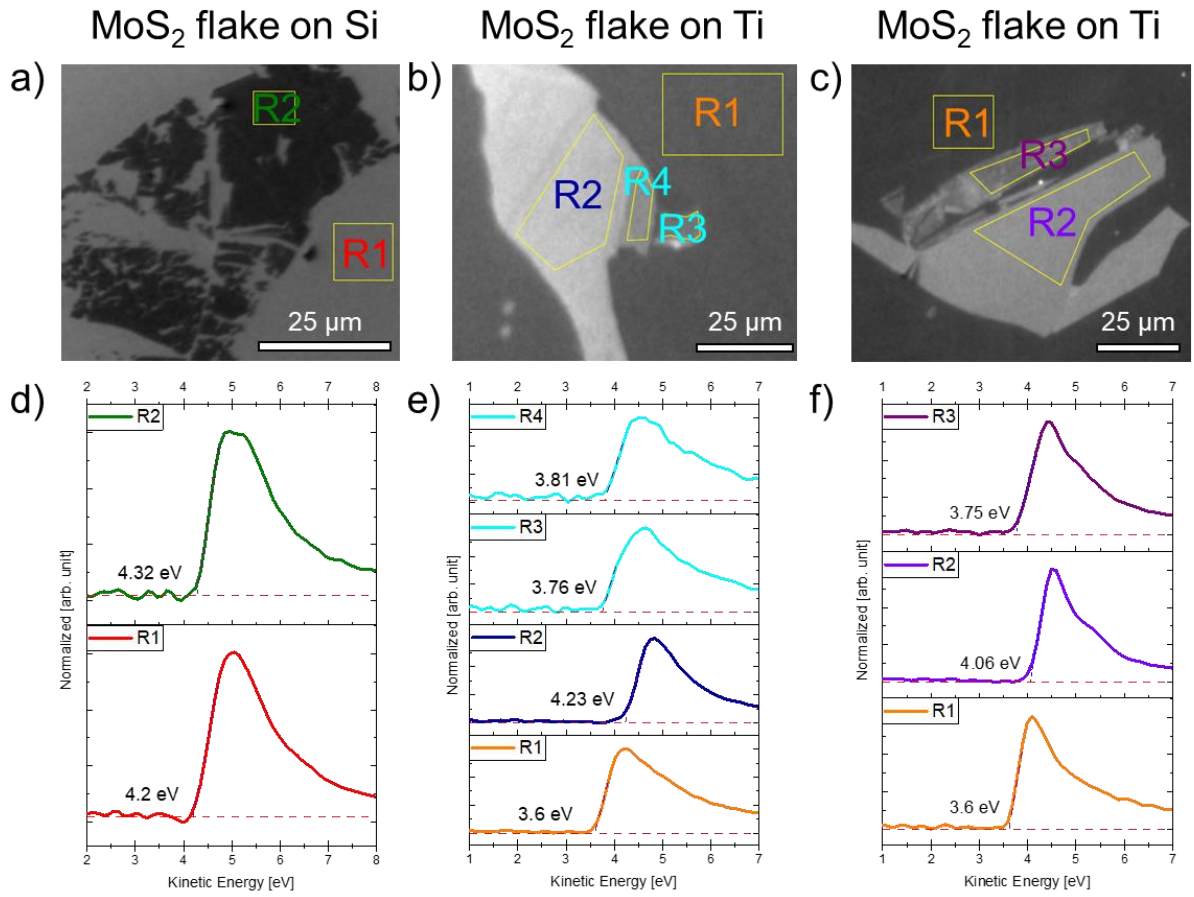

Figure 2 Average intensity images of work function contrast measurements for flake 1, flake 2 and flake 3 are shown in a), b) and c) respectively. Below the respective mean spectra for selected regions of interest are shown (d) – f)).

First, we will discuss the work function contrast of selected MoS_2 flakes prepared on naturally oxidized silicon and titanium substrates. In the following, we will refer to the flake on the oxidized silicon substrate (**Figure 2a, d** and **Fig. S3, Fig. S4c**) as flake 1, while the two flakes on the titanium substrates are referred to as flake 2 (**Figure 2b, e** and **Fig. S2, Fig. S4a**) and flake 3 (**Figure 2c, f** and **Fig. S1, Fig. S4b**). **Figure 2** shows PEEM images (the total diameter

of the field of view is 126 µm for the measured circular images, the figures shown are cutouts and the scales are adjusted accordingly) together with the normalized µ-PES spectra of the secondary electron cutoff. Regions of interest (denoted R1 - R4 in **Figure 2**) were selected based on previously acquired optical microscope images and observable color variations (**Figure S4**). Average spectra in **Figure 2d-f** were generated over all pixels in the chosen regions marked in **Figures 2a-c**. For a better comparison of the work functions, we measured the secondary electron cutoff from the pure substates with ultraviolet photoelectron spectroscopy (UPS) at our laboratory spectrometer. We found a work function of 4.2 eV and 3.6 eV for the silicon and titanium substrates, respectively (**Figure S3g**). This difference is in good agreement with literature data and the relative differences we found in our PEEM measurements on the substrate. Therefore, we referenced the work functions of the substrates to those value and adjusted the values for the MoS_2 flake regions based on the relative differences.

We find almost the same work function for the pristine titanium substrate regions (R1) for flake 2 and flake 3 and a higher work function for the silicon substrate of flake 1. A comparably high work function Φ is expected for MoS_2, a value of 5.4 eV was recently reported for single crystalline bulk substrates.[33] However, for monolayer or few-layers on oxidized silicon, significantly lower values were observed (Φ ~ 4.5 eV) by both PEEM and Kelvin probe force microscopy (KPFM).[48, 50, 51] We note that KPFM measures relative work functions, which may complicate a direct comparison of absolute values. Furthermore, a comparison to literature data has to take into account difference in the preparation method, the influence of contaminations in the case of measurements under ambient conditions,[50] as well as the choice of the substrate, which may alter the work function of MoS_2 flakes by several tenths of eV.[51] However and most importantly, all methods agree in that the work function increases from single to few-layer MoS_2.[48, 51, 52] Using PEEM under UHV conditions, for MoS_2 on oxidized silicon differences of 60 meV and 80 meV were observed for 1→2 and 2→3 monolayers, respectively. Thus, the

lower work function of regions R3 and R4 in **Figure 2b, c** clearly indicates a lower number of MoS_2 layers.

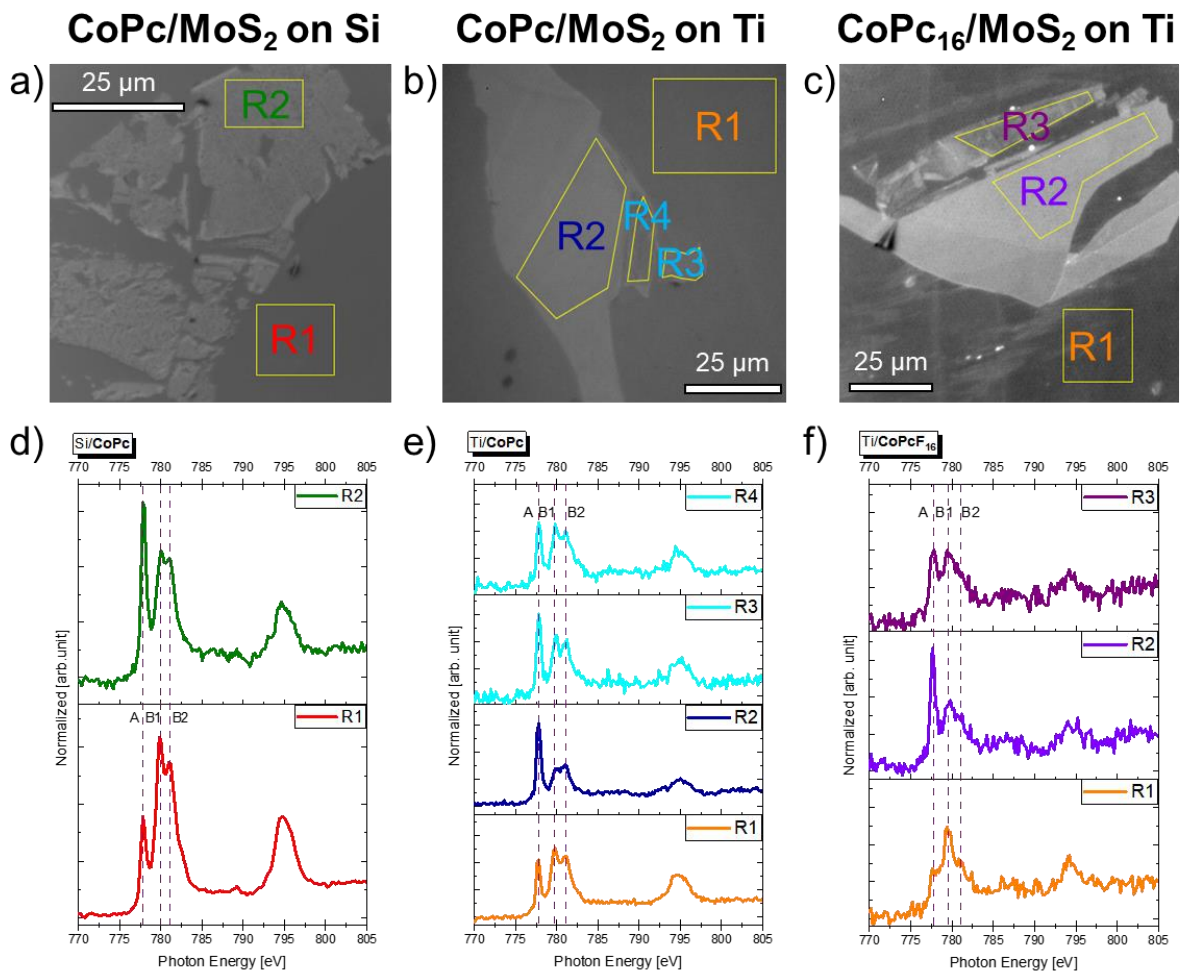

Figure 3 PEEM XAS measurements at an incident angle of 25° in the region of the Co L edge. a) - c) show average intensity images and selected regions of interests in these images. d) - f) show the normalized spectra of the respective ROI for the flakes 1 - 3 above.

In a next step, we deposited CoPc on flakes 1 and 2 and $CoPcF_{16}$ on flake 3. The corresponding PEEM images together with the averaged Co L_3 edge spectra of the selected regions are shown in **Figure 3**. The XAS spectra in **Figure 3d-f** were obtained by the analysis of PEEM images taken at different excitation energies. Generally, the XAS features discussed in **Figure 1** are also visible in the µ-XAS spectra of **Figure 3**. Due to the fixed measurement geometry all spectra were taken at an incident angle of 25° with respect to the surface of the sample. This is relatively close to the grazing incidence angle for the measurements of CoPc

and $CoPcF_{16}$ on bulk MoS_2 single crystals (20°). Thus, for preferred flat-lying molecules only a slight increase of the relative intensity of the in-plane polarized features B1 and B2 might be expected compared to bulk MoS_2 single crystals, discussed in **Figure 1** (cf. e.g. Refs.[34, 42] for the angular dependence of Co L_3 spectra). A further reason for a slightly increased intensity of B1 and B2 could be a different degree of the polarization of the synchrotron light. Considering these minor technical limitations, the μ-XAS spectra of CoPc and $CoPcF_{16}$ on large MoS_2 terraces (R2) in **Figure 3** are very similar to the related spectra on bulk MoS_2 single crystals at grazing incidence (20°) in **Figure 1**. In both cases, the out-of-plane polarized feature A clearly dominates the spectrum. In contrast, on the oxidized silicon and titanium surfaces (regions R1 in **Figure 3**), the molecules grow obviously in a different manner: The dominating in-plane features B1 and B2 indicate a preferred standing (edge-on) adsorption geometry, which can be related to the weaker molecule-substrate interaction with increasing (micro-)roughness of the substrates (i.e. the substrates are not atomically flat). Such effects were reported for different molecules (see, e.g. Refs. [29, 36]). Most importantly, the ratio of A/B intensities of the Co L_3 spectra for the regions R3 and R4 deviate distinctly from the regions R2 of the MoS_2 flakes on oxidized titanium (**Figure 3 e, f**), indicating significant tilt angles of the molecules to the surface plane or a disordered growth. This effect is observed to some weaker extent also on the region R2 on oxidized silicon (**Figure 3d**), where **Figure 3a** suggests a more inhomogeneous MoS_2 layer. The regions R3 and R4 are characterized by i) a lower number of MoS_2 layers and ii) by a smaller size compared to regions R2. Both could affect the molecular orientation of the deposited CoPc or $CoPcF_{16}$ molecules. The lower number of MoS_2 layers may affect the surface energy of the substrate, and the flexibility of the thin-layer MoS_2 may cause a certain corrugation due to the alignment at the substrate surface. The small lateral size of the thin MoS_2 regions might limit the favorable flat-lying adsorption geometry to a certain number of molecules and step-edge effects might become important. Further investigation is needed to understand the different adsorption geometry of Co phthalocyanines on smaller MoS_2 terraces.

In conclusion, we found that the orientation of cobalt phthalocyanines on technically relevant, small-sized thin-layers of MoS_2 flakes is significantly different compared to bulk MoS_2. This demonstrates that the molecular orientation on small sized (monolayer) TMDC flakes cannot be simply deduced from the orientation of organic molecules on related bulk substrates. For the understanding of electronic and optic interactions at such interfaces, different molecular orientations should be considered. From our perspective, especially the situation between electrodes with small distances seems to be critical, in particular if the evaporation of molecules occurs after the deposition of electrode structures.

Experimental Section

Cobalt phthalocyanine (CoPc, Sigma-Aldrich Chemie GmbH) and perfluorinated cobalt phthalocyanine ($CoPcF_{16}$, Sigma-Aldrich Chemie GmbH) were deposited on bulk MoS_2 (2D semiconductors Inc. USA) by thermal evaporation under ultra-high vacuum (UHV) conditions (base pressure about $1 \cdot 10^{-9}$ mbar). The evaporation chamber was directly attached to the spectrometer chamber. The nominal film thickness was determined using a quartz crystal microbalance, setting the mass density of CoPc and $CoPcF_{16}$ at 1.6 g/cm^3 and 1.8 g/cm^3, respectively, and checked by the comparison of XPS peak areas for bulk samples.

For experiments on bulk 2H-phase MoS_2, the crystals were cleaved by adhesive tape in UHV. The cleanliness was checked by X-ray photoelectron spectroscopy (XPS). These experiments were conducted at the PM4 beamline of the BESSY II electron storage ring operated by the Helmholtz-Zentrum Berlin (HZB) using the LowDosePES endstation.[53] Polarization-dependent X-ray absorption spectroscopy (XAS) measurements at the N K and Co L edges were carried out in total electron yield mode measuring the sample drain current and orienting the sample at different polar angles with respect to the incoming beam of fixed horizontal polarization. The correction for beamline characteristics of the photon flux was carried out using the drain current

from the last beamline mirror or XAS spectra of pristine gold substrates. The XAS spectra were normalized to the same step height well above the absorption edge.

For determining the orientation of CoPc and $CoPcF_{16}$ on MoS_2 flakes, laterally resolved spectromicroscopy experiments in a PEEM were conducted at IQMT's soft x-ray beamline WERA at the KIT Light Source, Karlsruhe, Germany. The degree of linear polarization was set to nominal values between 72 and 93%, all giving sufficient orientational contrast of the Co L edge with photon energies between 770 eV – 800 eV, the energy resolution was set to 490 meV. The FOCUS-PEEM (FOCUS GmbH) operates in a fixed geometry; the angle between the p-polarized incident photon beam and the normal of the sample was 65°. Since the fixed geometry does not allow a direct determination of the molecular orientation, the adsorption geometry was estimated from the known angular dependence of polarization dependent XAS spectra (measured e.g. on bulk MoS_2).

MoS2 flakes, containing regions with varying numbers of layers, were prepared for PEEM measurements using the top-down scotch tape method, starting with bulk MoS_2.[54] Exfoliated flakes were transferred onto a polydimethylsiloxane stamp (PF Gel Film®, Teltec GmbH). The stamp is pressed onto substrates, leaving thin-layers of TMDC on them. Mentioned substrates were commercially available silicon wafers, either coated with a 50 nm layer of titanium or used as purchased. To fit the dimensions of the PEEM sample holders, 7.5 x 7.5 mm substrates were cut from these wafers. Native titanium oxide and silicon oxide layers were found on both surfaces as evidenced by photoelectron emission measurements (Figure S1-3, Supporting Information). The substrates were ultrasonically cleaned with a solvent cascade, starting with acetone, followed by hexane, ethyl acetate, and isopropanol. As a final cleaning step, the substrates were placed in a UV oven (Photo Surface Processor PL16-110B-1, Sen Lights Corp) for 15 minutes. Successful transfers of the MoS_2 flakes were evaluated by optical microscope images. As this preparation method yields a large number of flakes with different thicknesses on the substrates, we selected the most promising ones based on contrast assessments. The

images of the for later experiments selected flakes are shown in Figure S4. Prior to the deposition of phthalocyanines, the samples were annealed under UHV conditions to 250 °C for 12 h to remove contamination from preparation and ensure a clean surface, as verified by PEEM measurements (see Figure S1-3).

ACKNOWLEDGMENTS

The authors thank the Helmholtz-Zentrum Berlin (electron storage ring BESSY II) for provision of synchrotron radiation at the beamline PM4. Financial travel support by HZB is thankfully acknowledged. The authors are grateful to the KIT Light Source, Karlsruhe, Germany, for the provision of beamtime. The Center for Light-Matter Interaction, Sensors & Analytics (LISA$^+$) at the University of Tübingen is acknowledged for technical support and Fabian Strauß for the preparation of the substrates. The work was supported by the German Research Council (PE 546/17-1, SCHE1905/9-1 (project no. 426008387)) and the European Research Council (ERC) under the European Union's Horizon 2020 research and innovation program (Grant Agreement 802822).

ASSOCIATED CONTENT

Supporting Information

Figure S1 Micro-XPS measurements on a MoS_2 flake on a titanium coated substrate. The intensity maps show the summed intensity measured over the S2p region (a), the Ti3p region (b) and the Mo3d region (c). The bright pixels have an overall high intensity while the intensity in darker areas is low. Below each image the average spectra, integrated over the total detector area is shown.

Figure S2 Micro-XPS measurements on a MoS_2 flake on a titanium coated substrate. The intensity maps show the summed intensity measured over the S2p region (a), the Ti3p region (b) and the Mo3d region (c). The bright pixels have an overall high intensity while the intensity

in darker areas is low. Below each image the average spectra, integrated over the total detector area is shown.

Figure S3 Micro-XPS measurements on a MoS_2 flake on native oxide silicon substrate. The intensity maps show the summed intensity measured over the S2p region (a), the Si2p region (b) and the Mo3d region (c). The bright pixels have an overall high intensity while the intensity in darker areas is low. Below each image the average spectra, integrated over the total detector area is shown.

Figure S4 Optical microscope images (500x magnification) of MoS_2 flakes on Ti (a) and b)) and on Si substrates (c)).

Figure S5 Angle dependent XAS measurements of a) N K edge region of clean bulk MoS_2 (red) and bulk MoS_2 with an overlayer of $CoPcF_{16}$ (black) b) N K edge region after the second deposition of $CoPcF_{16}$.

Figure S6 Measured BIAS voltages for flakes 1-3 (a) - c)) and the averaged spectra from the marked region of interest (d) – f)). g) measured secondary electron cutoff for the clean substrates

References

(1) Zeng, S. F.; Tang, Z. W.; Liu, C. S.; Zhou, P. Electronics based on two-dimensional materials: Status and outlook. *Nano Research* **2021**, *14* (6), 1752-1767. DOI: 10.1007/s12274-020-2945-z.

(2) Fiori, G.; Bonaccorso, F.; Iannaccone, G.; Palacios, T.; Neumaier, D.; Seabaugh, A.; Banerjee, S. K.; Colombo, L. Electronics based on two-dimensional materials. *Nat. Nanotechnol.* **2014**, *9* (10), 768-779. DOI: 10.1038/nnano.2014.207.

(3) Zheng, L.; Wang, X. W.; Jiang, H. J.; Xu, M. Z.; Huang, W.; Liu, Z. Recent progress of flexible electronics by 2D transition metal dichalcogenides. *Nano Research* **2022**, *15* (3), 2413-2432. DOI: 10.1007/s12274-021-3779-z.

(4) Manzeli, S.; Ovchinnikov, D.; Pasquier, D.; Yazyev, O. V.; Kis, A. 2D transition metal dichalcogenides. *Nature Reviews Materials* **2017**, *2* (8), 17033. DOI: 10.1038/natrevmats.2017.33.

(5) Novoselov, K. S.; Jiang, D.; Schedin, F.; Booth, T. J.; Khotkevich, V. V.; Morozov, S. V.; Geim, A. K. Two-dimensional atomic crystals. *Proceedings of the National Academy of Sciences* **2005**, *102* (30), 10451-10453. DOI: 10.1073/pnas.0502848102 (acccessed 2023/01/19).

(6) Wang, Q. H.; Kalantar-Zadeh, K.; Kis, A.; Coleman, J. N.; Strano, M. S. Electronics and optoelectronics of two-dimensional transition metal dichalcogenides. *Nat. Nanotechnol.* **2012**, *7* (11), 699-712, Review. DOI: 10.1038/nnano.2012.193.
(7) Radisavljevic, B.; Radenovic, A.; Brivio, J.; Giacometti, V.; Kis, A. Single-layer MoS2 transistors. *Nat. Nanotechnol.* **2011**, *6* (3), 147-150. DOI: 10.1038/nnano.2010.279.
(8) Liu, Y.; Weiss, N. O.; Duan, X. D.; Cheng, H. C.; Huang, Y.; Duan, X. F. Van der Waals heterostructures and devices. *Nature Reviews Materials* **2016**, *1* (9). DOI: 10.1038/natrevmats.2016.42.
(9) Pham, P. V.; Bodepudi, S. C.; Shehzad, K.; Liu, Y.; Xu, Y.; Yu, B.; Duan, X. F. 2D Heterostructures for Ubiquitous Electronics and Optoelectronics: Principles, Opportunities, and Challenges. *Chem. Rev.* **2022**, *122* (6), 6514-6613. DOI: 10.1021/acs.chemrev.1c00735.
(10) Nevola, D.; Hoffman, B. C.; Bataller, A.; Ade, H.; Gundogdu, K.; Dougherty, D. B. Rigid valence band shift due to molecular surface counter-doping of MoS2. *Surf. Sci.* **2019**, *679*, 254-258, Article. DOI: 10.1016/j.susc.2018.09.016.
(11) Jing, Y.; Tan, X.; Zhou, Z.; Shen, P. W. Tuning electronic and optical properties of MoS2 monolayer via molecular charge transfer. *Journal of Materials Chemistry A* **2014**, *2* (40), 16892-16897, Article. DOI: 10.1039/c4ta03660c.
(12) Park, S.; Schultz, T.; Xu, X. M.; Wegner, B.; Aljarb, A.; Han, A.; Li, L. J.; Tung, V. C.; Amsalem, P.; Koch, N. Demonstration of the key substrate-dependent charge transfer mechanisms between monolayer MoS2 and molecular dopants. *Commun. Phys.* **2019**, *2*, 8, Article. DOI: 10.1038/s42005-019-0212-y.
(13) Huang, Y. L.; Zheng, Y. J.; Song, Z. B.; Chi, D. Z.; Wee, A. T. S.; Quek, S. Y. The organic-2D transition metal dichalcogenide heterointerface. *Chemical Society Reviews* **2018**, *47* (9), 3241-3264, Review. DOI: 10.1039/c8cs00159f.
(14) Amsterdam, S. H.; Marks, T. J.; Hersam, M. C. Leveraging Molecular Properties to Tailor Mixed-Dimensional Heterostructures beyond Energy Level Alignment. *J Phys Chem Lett* **2021**, *12* (19), 4543-4557, Article. DOI: 10.1021/acs.jpclett.1c00799.
(15) Amsterdam, S. H.; Stanev, T. K.; Wang, L. Q.; Zhou, Q. F.; Irgen-Gioro, S.; Padgaonkar, S.; Murthy, A. A.; Sangwan, V. K.; Dravid, V. P.; Weiss, E. A.; et al. Mechanistic Investigation of Molybdenum Disulfide Defect Photoluminescence Quenching by Adsorbed Metallophthalocyanines. *J. Am. Chem. Soc.* **2021**, *143* (41), 17153-17161, Article. DOI: 10.1021/jacs.1c07795.
(16) Krumland, J.; Cocchi, C. Conditions for electronic hybridization between transition-metal dichalcogenide monolayers and physisorbed carbon-conjugated molecules. *Electronic Structure* **2021**, *3* (4), 044003. DOI: 10.1088/2516-1075/ac421f.
(17) Casotto, A.; Drera, G.; Perilli, D.; Freddi, S.; Pagliara, S.; Zanotti, M.; Schio, L.; Verdini, A.; Floreano, L.; Di Valentin, C.; Sangaletti, L. pi-Orbital mediated charge transfer channels in a monolayer Gr-NiPc heterointerface unveiled by soft X-ray electron spectroscopies and DFT calculations. *Nanoscale* **2022**, *14* (36), 13166-13177. DOI: 10.1039/d2nr02647c.
(18) Koch, N. Opportunities for energy level tuning at inorganic/organic semiconductor interfaces. *Applied Physics Letters* **2021**, *119* (26), 260501. DOI: 10.1063/5.0074963 (acccessed 2023/01/10).
(19) Duhm, S.; Heimel, G.; Salzmann, I.; Glowatzki, H.; Johnson, R. L.; Vollmer, A.; Rabe, J. P.; Koch, N. Orientation-dependent ionization energies and interface dipoles in ordered molecular assemblies. *Nature Materials* **2008**, *7* (4), 326-332. DOI: 10.1038/nmat2119.
(20) Forrest, S. R. Ultrathin organic films grown by organic molecular beam deposition and related techniques. *Chem. Rev.* **1997**, *97* (6), 1793-1896, Review. DOI: 10.1021/cr941014o.
(21) Kudo, K.; Wang, D. X.; Iizuka, M.; Kuniyoshi, S.; Tanaka, K. Schottky gate static induction transistor using copper phthalocyanine films. *Thin Solid Films* **1998**, *331* (1-2), 51-54. DOI: 10.1016/S0040-6090(98)00945-6.
(22) Bao, Z.; Lovinger, A. J.; Dodabalapur, A. Organic field-effect transistors with high mobility based on copper phthalocyanine. *Appl. Phys. Lett.* **1996**, *69* (20), 3066-3068. DOI: Doi 10.1063/1.116841.

(23) Melville, O. A.; Lessard, B. H.; Bender, T. P. Phthalocyanine-Based Organic Thin-Film Transistors: A Review of Recent Advances. *ACS Applied Materials & Interfaces* **2015**, *7* (24), 13105-13118. DOI: 10.1021/acsami.5b01718.
(24) Greulich, K.; Belser, A.; Basova, T.; Chassé, T.; Peisert, H. Interfaces between Different Iron Phthalocyanines and Au(111): Influence of the Fluorination on Structure and Interfacial Interactions. *J. Phys. Chem. C* **2022**, *126* (1), 716-727, Article. DOI: 10.1021/acs.jpcc.1c08826.
(25) Zhou, Q. F.; Liu, Z. F.; Marks, T. J.; Darancet, P. Electronic Structure of Metallophthalocyanines, MPc (M = Fe, Co, Ni, Cu, Zn, Mg) and Fluorinated MPc. *Journal of Physical Chemistry A* **2021**, *125* (19), 4055-4061. DOI: 10.1021/acs.jpca.0c10766.
(26) Toader, M.; Gopakumar, T. G.; Shukrynau, P.; Hietschold, M. Exploring the F16CoPc/Ag(110) Interface Using Scanning Tunneling Microscopy and Spectroscopy. 2. Adsorption-Induced Charge Transfer Effect. *J. Phys. Chem. C* **2010**, *114* (49), 21548-21554, Article. DOI: 10.1021/jp1078295.
(27) Peisert, H.; Knupfer, M.; Schwieger, T.; Fuentes, G. G.; Olligs, D.; Fink, J.; Schmidt, T. Fluorination of copper phthalocyanines: Electronic structure and interface properties. *J. Appl. Phys.* **2003**, *93* (12), 9683-9692. DOI: Doi 10.1063/1.1577223.
(28) Balle, D.; Adler, H.; Grüninger, P.; Karstens, R.; Ovsyannikov, R.; Giangrisostomi, E.; Chassé, T.; Peisert, H. Influence of the Fluorination of CoPc on the Interfacial Electronic Structure of the Coordinated Metal Ion. *J. Phys. Chem. C* **2017**, *121* (34), 18564-18574. DOI: 10.1021/acs.jpcc.7b04494.
(29) Peisert, H.; Biswas, I.; Knupfer, M.; Chassé, T. Orientation and electronic properties of phthalocyanines on polycrystalline substrates. *Phys Status Solidi B* **2009**, *246* (7), 1529-1545. DOI: DOI 10.1002/pssb.200945051.
(30) Peisert, H.; Schwieger, T.; Auerhammer, J. M.; Knupfer, M.; Golden, M. S.; Fink, J.; Bressler, P. R.; Mast, M. Order on disorder: Copper phthalocyanine thin films on technical substrates. *J. Appl. Phys.* **2001**, *90* (1), 466-469.
(31) Kera, S.; Casu, M. B.; Bauchspiess, K. R.; Batchelor, D.; Schmidt, T.; Umbach, E. Growth mode and molecular orientation of phthalocyanine molecules on metal single crystal substrates: A NEXAFS and XPS study. *Surf. Sci.* **2006**, *600* (5), 1077-1084, Article. DOI: 10.1016/j.susc.2005.12.042.
(32) Padgaonkar, S.; Amsterdam, S. H.; Bergeron, H.; Su, K.; Marks, T. J.; Hersam, M. C.; Weiss, E. A. Molecular-Orientation-Dependent Interfacial Charge Transfer in Phthalocyanine/MoS2 Mixed-Dimensional Heterojunctions. *J. Phys. Chem. C* **2019**, *123* (21), 13337-13343. DOI: 10.1021/acs.jpcc.9b04063.
(33) Greulich, K.; Belser, A.; Bölke, S.; Grüninger, P.; Karstens, R.; Sättele, M. S.; Ovsyannikov, R.; Giangrisostomi, E.; Basova, T. V.; Klyamer, D. D.; et al. Charge Transfer from Organic Molecules to Molybdenum Disulfide: Influence of the Fluorination of Iron Phthalocyanine. *J. Phys. Chem. C* **2020**, *124* (31), 16990-16999. DOI: 10.1021/acs.jpcc.0c03862.
(34) Peisert, H.; Uihlein, J.; Petraki, F.; Chassé, T. Charge transfer between transition metal phthalocyanines and metal substrates: The role of the transition metal. *J. Electron Spectros. Relat. Phenomena* **2015**, *204*, 49-60. DOI: 10.1016/j.elspec.2015.01.005.
(35) Scardamaglia, M.; Struzzi, C.; Lizzit, S.; Dalmiglio, M.; Lacovig, P.; Baraldi, A.; Mariani, C.; Betti, M. G. Energetics and Hierarchical Interactions of Metal Phthalocyanines Adsorbed on Graphene/Ir(111). *Langmuir* **2013**, *29* (33), 10440-10447, Article. DOI: 10.1021/1a401850v.
(36) Breuer, T.; Salzmann, I.; Gotzen, J.; Oehzelt, M.; Morherr, A.; Koch, N.; Witte, G. Interrelation between Substrate Roughness and Thin-Film Structure of Functionalized Acenes on Graphite. *Crystal Growth & Design* **2011**, *11* (11), 4996-5001. DOI: 10.1021/cg200894y.
(37) Schmidt, T.; Wilkens, T.; Falta, J. Ordering of copper phthalocyanine films on functionalized Si(111). *Surf. Sci.* **2022**, *725*, 11, Article. DOI: 10.1016/j.susc.2022.122127.
(38) Cranston, R. R.; Lessard, B. H. Metal phthalocyanines: thin-film formation, microstructure, and physical properties. *RSC Advances* **2021**, *11* (35), 21716-21737. DOI: 10.1039/d1ra03853b.

(39) Evans, D. A.; Steiner, H. J.; Vearey-Roberts, A. R.; Bushell, A.; Cabailh, G.; O'Brien, S.; Wells, J. W.; McGovern, I. T.; Dhanak, V. R.; Kampen, T. U.; et al. Synchrotron radiation studies of inorganic-organic semiconductor interfaces. *Nuclear Instruments & Methods in Physics Research Section B-Beam Interactions with Materials and Atoms* **2003**, *199*, 475-480. DOI: 10.1016/s0168-583x(02)01595-1.
(40) Stöhr, J. *NEXAFS Spectroscopy*; Springer, 1992.
(41) Stöhr, J.; Outka, D. A. Determination of molecular orientations on surfaces from the angular dependence of near-edge x-ray-absorption fine-structure spectra. *Phys Rev B* **1987**, *36* (15), 7891-7905. DOI: 10.1103/PhysRevB.36.7891.
(42) Kroll, T.; Aristov, V. Y.; Molodtsova, O. V.; Ossipyan, Y. A.; Vyalikh, D. V.; Büchner, B.; Knupfer, M. Spin and orbital ground state of Co in cobalt phthalocyanine. *J Phys Chem A* **2009**, *113* (31), 8917-8922. DOI: 10.1021/jp903001v.
(43) de Groot, F. Multiplet effects in X-ray spectroscopy. *Coord. Chem. Rev.* **2005**, *249* (1-2), 31-63, Review. DOI: 10.1016/j.ccr.2004.03.018.
(44) Zhang, T.; Brumboiu, I. E.; Lanzilotto, V.; Luder, J.; Grazioli, C.; Giangrisostomi, E.; Ovsyannikov, R.; Sass, Y.; Bidermane, I.; Stupar, M.; et al. Conclusively Addressing the CoPc Electronic Structure: A Joint Gas-Phase and Solid-State Photoemission and Absorption Spectroscopy Study. *J. Phys. Chem. C* **2017**, *121* (47), 26372-26378, Article. DOI: 10.1021/acs.jpcc.7b08524.
(45) Brumboiu, I. E.; Haldar, S.; Luder, J.; Eriksson, O.; Herper, H. C.; Brena, B.; Sanyal, B. Influence of Electron Correlation on the Electronic Structure and Magnetism of Transition-Metal Phthalocyanines. *Journal of Chemical Theory and Computation* **2016**, *12* (4), 1772-1785. DOI: 10.1021/acs.jctc.6b00091.
(46) Belser, A.; Greulich, K.; Grüninger, P.; Karstens, R.; Ovsyannikov, R.; Giangrisostomi, E.; Nagel, P.; Merz, M.; Schuppler, S.; Chassé, T.; Peisert, H. Perfluorinated Phthalocyanines on Cu(110) and Cu(110)-(2 × 1)O: The Special Role of the Central Cobalt Atom. *J. Phys. Chem. C* **2021**, *125* (16), 8803-8814. DOI: 10.1021/acs.jpcc.1c01215.
(47) Keyshar, K.; Berg, M.; Zhang, X.; Vajtai, R.; Gupta, G.; Chan, C. K.; Beechem, T. E.; Ajayan, P. M.; Mohite, A. D.; Ohta, T. Experimental Determination of the Ionization Energies of MoSe2, WS2, and MoS2 on SiO2 Using Photoemission Electron Microscopy. *Acs Nano* **2017**, *11* (8), 8223-8230. DOI: 10.1021/acsnano.7b03242.
(48) Berg, M.; Keyshar, K.; Bilgin, I.; Liu, F. Z.; Yamaguchi, H.; Vajtai, R.; Chan, C.; Gupta, G.; Kar, S.; Ajayan, P.; et al. Layer dependence of the electronic band alignment of few-layer MoS2 on SiO2 measured using photoemission electron microscopy. *Phys Rev B* **2017**, *95* (23). DOI: 10.1103/PhysRevB.95.235406.
(49) Fregnaux, M.; Kim, H.; Rouchon, D.; Derycke, V.; Bleuse, J.; Voiry, D.; Chhowalla, M.; Renault, O. Chemistry and electronics of single layer MoS2 domains from photoelectron spectromicroscopy using laboratory excitation sources. *Surf. Interface Anal.* **2016**, *48* (7), 465-469. DOI: 10.1002/sia.5992.
(50) Ochedowski, O.; Marinov, K.; Scheuschner, N.; Poloczek, A.; Bussmann, B. K.; Maultzsch, J.; Schleberger, M. Effect of contaminations and surface preparation on the work function of single layer MoS2. *Beilstein Journal of Nanotechnology* **2014**, *5*, 291-297, Article. DOI: 10.3762/bjnano.5.32.
(51) Lattyak, C.; Gehrke, K.; Vehse, M. Layer-Thickness-Dependent Work Function of MoS2 on Metal and Metal Oxide Substrates. *J. Phys. Chem. C* **2022**, *126* (32), 13929-13935. DOI: 10.1021/acs.jpcc.2c03268.
(52) Tamulewicz, M.; Kutrowska-Girzycka, J.; Gajewski, K.; Serafinczuk, J.; Sierakowski, A.; Jadczak, J.; Bryja, L.; Gotszalk, T. P. Layer number dependence of the work function and optical properties of single and few layers MoS2: effect of substrate. *Nanotechnology* **2019**, *30* (24). DOI: 10.1088/1361-6528/ab0caf.
(53) Giangrisostomi, E.; Ovsyannikov, R.; Sorgenfrei, F.; Zhang, T.; Lindblad, A.; Sassa, Y.; Cappel, U. B.; Leitner, T.; Mitzner, R.; Svensson, S.; et al. Low Dose Photoelectron Spectroscopy at BESSY II: Electronic structure of matter in its native state. *J. Electron Spectros. Relat. Phenomena* **2018**, *224*, 68-78. DOI: https://doi.org/10.1016/j.elspec.2017.05.011.

(54) Novoselov, K. S.; Castro Neto, A. H. Two-dimensional crystals-based heterostructures: materials with tailored properties. *Physica Scripta* **2012**, *T146* (T146), 014006. DOI: 10.1088/0031-8949/2012/T146/014006.